Femtosecond water dynamics in reverse-micellar nanodroplets

Cringus, D; Lindner, J; Milder, MTW; Pshenichnikov, MS; Vohringer, P; Wiersma, DA; Milder, Maaike T.W.; Pshenichnikov, Maxim S.; Vöhringer, Peter

Published in:
Chemical Physics Letters

DOI:
10.1016/j.cplett.2005.04.020

Publication date:
2005

Available online at www.sciencedirect.com
SCIENCE DIRECT®
Chemical Physics Letters 408 (2005) 162–168
CHEMICAL PHYSICS LETTERS
www.elsevier.com/locate/cplett

Femtosecond water dynamics in reverse-micellar nanodroplets

Dan Cringus [a], Jörg Lindner [b], Maaike T.W. Milder [a], Maxim S. Pshenichnikov [a,*], Peter Vöhringer [b], Douwe A. Wiersma [a]

[a] Department of Physical Chemistry, Materials Science Centre, University of Groningen, Nijenborgh 4, 9747 AG Groningen, The Netherlands
[b] Institut für Physikalische und Theoretische Chemie, Rheinische Friedrich-Wilhelms-Universität, Wegelerstraße 12, 53115 Bonn, Germany

Received 24 February 2005; in final form 5 April 2005
Available online 28 April 2005

Abstract

Vibrational energy relaxation and ultrafast thermalization following impulsive excitation of the OH-stretching band of water nanodroplets confined to reverse micelles is studied by infrared pump–probe spectroscopy with sub-100 fs time resolution. The self-consistent analysis of experimental data for micelles diameters ranging from 1 to 10 nm as well as for bulk water reveals distinctly different vibrational lifetimes for the water molecules in the bulk-like core (270 fs) and in the surfactant vicinity (800 fs), which is a direct proof of a strongly disturbed hydrogen-bond network.

The geometric confinement of liquid water is a central issue for a wide variety of research areas ranging from the materials to the life sciences [1,2]. In particular, aqueous droplets embedded in nanoporous hosts serve as perfectly size-adapted reaction media for the heterogeneous synthesis of novel semi-conducting colloidal materials with promising applications in optoelectronics [3]. Nanometer-dimensioned water inclusions such as water wires and pockets are key ingredients that determine the tertiary structure and, consequently, the function of proteins [2]. The quasi-two-dimensional confinement of water at membrane interfaces [4] is considered crucial to the dynamics of biological charge and mass transfer and hence, for the communication between cells or cell compartments [5]. As a model system of water under geometrically confined conditions, aqueous reverse micelles have recently raised considerable interest [6].

The reverse micellar L_2-phase of the ternary oil-surfactant–water mixtures is composed of nearly spherical nanometer-sized water droplets covered by a monolayer of amphiphilic surfactant, thereby immersing the otherwise immiscible pair of liquids. MD simulations show [7] that the structure of water in reverse micelles with radii larger than ~1 nm can be discussed in terms of bulk-like and AOT-bound water molecules (frequently called 'free' and 'bound' molecules, respectively, which might be misleading). Bulk-like water, found in the center of the micelle, has a hydrogen-bond network similar to bulk phase water. AOT-bound water, which forms a hydration layer of the polar surfactant head groups, is characterized by a strongly perturbed hydrogen-bond network as compared to the bulk.

Aqueous reverse micelles have been under extensive experimental scrutiny through a variety of experimental methods, e.g., nuclear magnetic resonance [8], THz spectroscopy [9], neutron scattering [10], linear infrared [11] and nonlinear ultrafast spectroscopy [12–19]. To date, most of the femtosecond time-resolved studies have concentrated on dynamics of a solvated chromophore such as a dye molecule [12,17], a small inorganic anion [13], a hydrated electron [14], or an HOD molecule in aqueous environment [20]. These experiments have confirmed the earlier conclusion that with a gradually increasing size of

* Corresponding author.
E-mail addresses: g.d.cringus@rug.nl (D. Cringus), m.s.pchenitchnikov@rug.nl (M.S. Pshenichnikov).

0009-2614/$ - see front matter © 2005 Elsevier B.V. All rights reserved.
doi:10.1016/j.cplett.2005.04.020

the micelle the properties of the confined water approach those of bulk water. Recently, ultrafast dynamics of H_2O in reverse micelles have been investigated by picosecond infrared [15,16] and by IR/anti-Stokes Raman [18] spectroscopy following direct excitation of the OH-stretching mode of water molecules. These experiments (especially the latter ones) revealed a number of fascinating and detailed insights into the process of heat transfer from the water droplet to the micelle exterior. However, they did not address water dynamics within the nanodroplets as the picosecond time resolution was insufficient to unravel such dynamics.

In this Letter, we report results of pump–probe experiments on vibrational energy relaxation in aqueous reverse micellar nanodroplets following an OH-stretching mode excitation with 70-fs mid-IR pulses. The high temporal resolution allows us to disentangle vibrational population relaxation, energy equilibration within the entrapped water pool and finally, heat flux away from the micelles into the surrounding oil phase. On the basis of the developed model we show that for large micelles enclosing tens of thousands of water molecules, the population dynamics are similar to those in bulk water. In the smallest micelles, which contain only tens of water molecules, the OH-stretch lifetime is considerably longer than in pure water but is still much shorter than that of highly diluted water of liquid binary mixtures [21–23]. Dynamics in intermediate-size micelles can be decomposed into independent contributions of these two limiting cases, which strongly suggests that the OH-lifetime is predominantly sensitive to interactions with nearest neighboring molecules.

Femtosecond IR pulses with a central wavelength of ~3 μm were generated in a standard chain of optical parametric amplifiers (OPA) pumped by a 1-kHz Ti:Sapphire system. The OPA output was split into an intense pump and a weak probe beam, both of which were then focused in the sample and subsequently dispersed by a monochromator to probe the dynamics at a selected frequency. The spectral content of the 70-fs pulses allowed for measuring pump–probe signals over a wide range of detection frequencies without tuning of the 3400 cm^{-1} central frequency of the pulses. For the experiments on bulk water the pump and probe pulses were derived from two independent OPAs to further enhance the spectral coverage. In this case, the pump duration was somewhat longer (~150 fs). The rotational-free signals were either measured directly under a magic angle (54.7°) geometry or recalculated from two orthogonally polarized probe scans according to Ref. [24]. The details of the anisotropy measurements are discussed elsewhere [19].

The micelles samples were prepared by shaking for several minutes mixtures of bis(2-ethylhexyl) sulfosuccinate sodium salt (AOT, SigmaUltra 99%), 2,2,4-trimethylpentane (isooctane, Aldrich 99.8%) and water (Aldrich, HPLC grade). Aqueous nanodroplets in the ternary mixture isooctane–H_2O–AOT are commonly characterized by the molar water-to-AOT ratio, $\mu = [H_2O]/[AOT]$, and the water mass fraction, $\alpha = m_{water}/m_{total}$ [6]. The former quantity defines the size of the entrapped water droplet whereas the latter determines the reverse micelles concentration. By adjusting the molar water-to-AOT ratio the properties of water can be continuously tuned from an aqueous nanometer-sized object to the aqueous bulk phase. The water mass fraction was $\alpha \sim 0.01$, resulting in optical density (OD) within 0.5–1.2. To avoid accumulation of thermal effects, the samples at room temperature were contained in a 100 μm thick free-standing jet; for bulk water a rotating cell with a sample thickness of 2 μm was used. We investigated the influence of a geometrical confinement on the vibrational dynamics of water by studying aqueous nanodroplets with $1 \leqslant \mu \leqslant 35$ corresponding to diameters ranging from 1 to 10 nm. For each reverse micelle size, the complete data set consists of pump–probe transients measured as a function of delay between pump and probe pulses up to 25 ps, and monochromator settings from 3100 to 3650 cm^{-1} with a step of 50 cm^{-1}. For small micelles ($\mu = 1$–2), the amount of free 'bulk-like' water is thought to vanish, for medium sizes ($\mu = 7$–10) there is an approximately equal number of bound and free water molecules in the nanodroplet, while for the largest micelles ($\mu = 35$) most of the water molecules belong to the aqueous bulk-like core [7]. The linear absorption spectra clearly illustrate this trend (Fig. 1). For very large micelles (Fig. 1, blue triangles), the absorption spectrum is almost identical to that of pure water (Fig. 1, pink diamonds and shaded contour). Decreasing the micelle diameter causes a blue shift of the spectrum (Fig. 1, green circles) indicating a strong perturbation of the hydrogen-bond network of

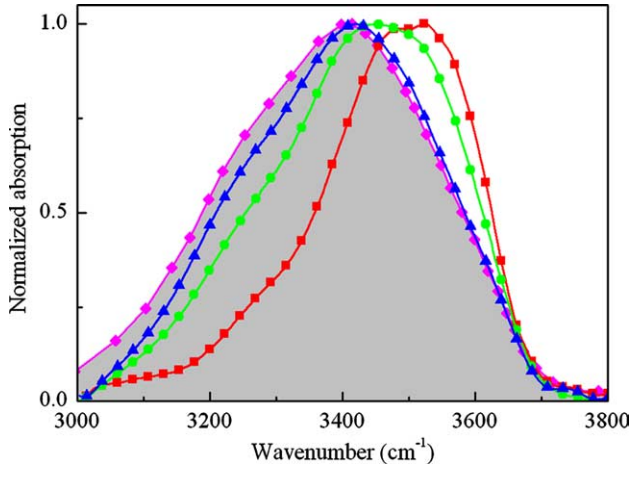

Fig. 1. OH-stretching band of bulk water (pink diamonds and shaded contour) and of water trapped in reverse micelles of sizes corresponding to $\mu = 35$ (blue triangles), $\mu = 10$ (green circles) and $\mu = 1$ (red squares). (For interpretation of the references to color in this figure legend, the reader is referred to the web version of this article.)

water molecules. The effect is even more pronounced when water is confined in the smallest micelles (Fig. 1, red squares) with yet even weaker hydrogen bonds formed presumably between water and AOT molecules. Breaking and weakening of the hydrogen bonds result in a distinct blue shift ($\sim$100 cm^{-1}) of the latter spectrum compared to that of the largest micelles.

Fig. 2a shows transient spectra for three representative micelle sizes at a pump–probe delay of 100 fs. These spectra are mostly related to the excited state, $|1\rangle$, of the OH-stretching mode because at such a short delay, its depopulation is negligible. All three signals are characterized by induced bleaching and stimulated emission of the $|0\rangle \rightarrow |1\rangle$ vibrational transition (maximum around 3500 cm^{-1}), and induced absorption of the $|1\rangle \rightarrow |2\rangle$ vibrational transition whose center frequency is shifted to $\sim$3200 cm^{-1} due to anharmonicity. However, a straightforward derivation of its value is not possible as the widths of ground-state and excited-state absorption contours are comparable to the anharmonic shift [21]. Note that the transient spectrum for the intermediate size micelles ($\mu = 10$) displays the largest red-shift. This is because nearly equal amounts of bound and free water are present in the micelle resulting in a maximum width of the corresponding linear absorption spectrum.

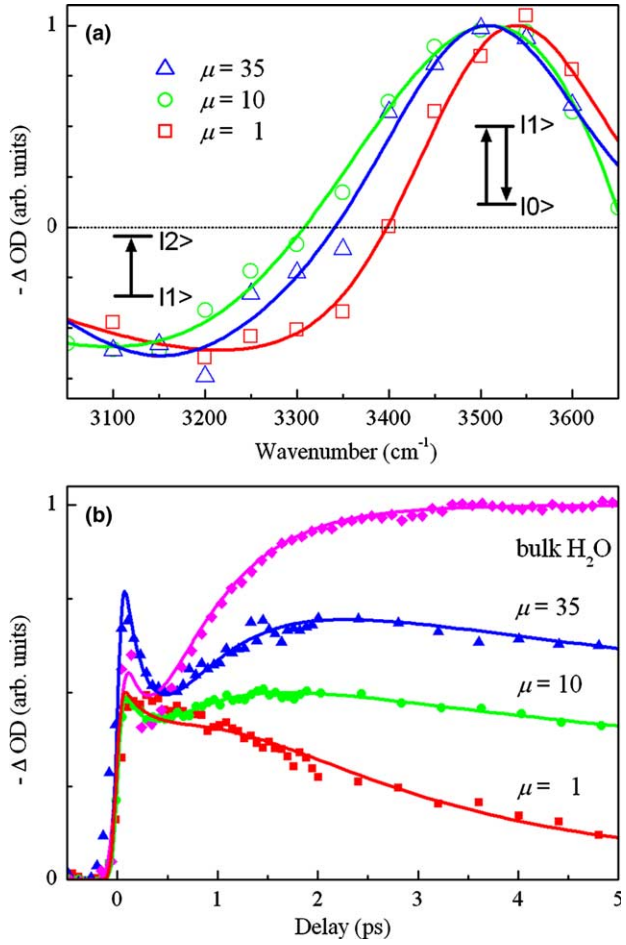

Fig. 2. Transient spectra at 100 fs delay (a) and pump–probe transients at the wavelength of 3450 cm^{-1} (b) for samples with $\mu = 1$ (red squares), $\mu = 10$ (green circles) and $\mu = 35$ (blue triangles), and bulk water (pink diamonds). The peak and the dip in (a) correspond to bleaching/emission at the $|0\rangle \rightarrow |1\rangle$ transition and induced absorption at the $|1\rangle \rightarrow |2\rangle$ transition, respectively, as schematically shown by diagrams. (For interpretation of the references to color in this figure legend, the reader is referred to the web version of this article.)

Several typical pump–probe transients are displayed in Fig. 2b. For all micelle diameters, the signal is characterized by a fast (several hundreds of femtoseconds) initial decay, followed by a rise on a sub-picosecond time scale and a final decay on a time scale of several picoseconds. The corresponding signal for bulk water levels off after a few picoseconds and then remains constant over our experimental time window. Therefore, the final decay of the pump–probe signals of reverse micelles is directly connected to the cooling of a micelle as a whole [16]. The cooling rate is higher for smaller micelles, as expected by classical heat diffusion. The intermediate signal growth has been assigned previously [25] to the excitation of low-frequency collective modes due to redistribution of the initially deposited energy. The corresponding temperature rise obtained from comparison of the transient spectra and the steady-state differential absorption spectra at elevated temperatures is roughly 10 K, in reasonable agreement with estimations made on the basis of excitation pulse energy, water heat capacity, and excited sample volume.

The analysis of the pump–probe data of aqueous nanodroplets is built on the kinetic model shown schematically in Fig. 3. The model generalizes the previously reported mechanism for energy equilibration in the aqueous bulk [25], and additionally introduces a heat conduction description for subsequent cooling of the micelles. The experimentally observed time scales (cf. Fig. 2b) require the model to invoke the three most relevant modes: the initially excited OH-stretching, $|i\rangle$ ($i = 0, 1, 2$), an intermediate, $|\text{int}\rangle$ and a thermally accessible mode, $|j_{\text{hot}}\rangle$ ($j = 0, 1$). After the pump pulse excites a fraction of the water molecules from the ground state $|0\rangle$ to the first excited state $|1\rangle$ of the OH-stretching

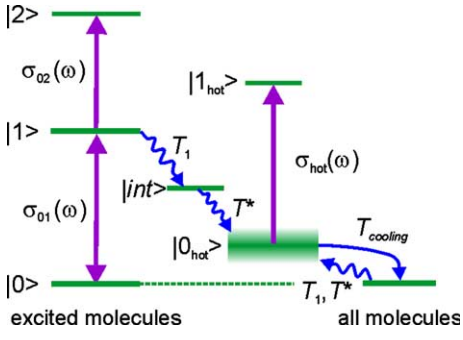

Fig. 3. Energy level diagram for the kinetic model.

vibration at time $t = 0$, the following processes occur: (i) the excited state population of the stretching mode $|1\rangle$ is transferred with a rate coefficient $1/T_1$ into the intermediate mode $|\text{int}\rangle$. (ii) Subsequently, the intermediate mode is depopulated with a rate constant $1/T^*$, resulting in energy equilibration over the low-frequency thermally activated modes, $|0_{\text{hot}}\rangle$, of the initially excited and surrounding water molecules. This process leaves the micelles at an elevated temperature. (iii) Finally, thermal relaxation due to heat diffusion from the micelle into the hydrophobic solvent results in local cooling with a decay of the micelle temperature. Hence, the proposed model describes a light-triggered temperature jump experiment, which takes into account a delayed perturbation resulting from the intermediate energy transfer (i) and redistribution (ii) events.

The rate equations yield the following expressions for the populations of the first excited state of the stretching mode and the thermally activated ground state, respectively:

$$N_1(t) = N_0 \mathrm{e}^{-t/T_1}, \tag{1}$$

$$N_{\text{hot}}(t) = N_0 \left[a(1 - \mathrm{e}^{-t/T_1}) + (1-a)\left(1 - \frac{T^* \mathrm{e}^{-t/T^*} - T_1 \mathrm{e}^{-t/T_1}}{T^* - T_1}\right)\right], \tag{2}$$

where N_0 is the fraction of the initially excited water molecules. The two terms in square brackets account for populating of the hot ground state either directly (with the probability a) or via an intermediate state (with the probability $1 - a$). The probe pulse monitors the changes of the averaged sample optical density according to

$$\Delta\text{OD}(\omega, t) \propto [\sigma_{12}(\omega) - 2\sigma_{01}(\omega)]N_1(t) + \frac{N_{\text{hot}}(t)}{N_0} \times N[\sigma_{\text{hot}}(\omega) - \sigma_{01}(\omega)][(\beta - 1)\mathrm{e}^{-t/T_{\text{cooling}}} + 1], \tag{3}$$

where $\sigma_{01}(\omega)$, $\sigma_{12}(\omega)$, and $\sigma_{\text{hot}}(\omega)$ are absorption cross-sections of the ground, excited and hot-ground states, respectively, and N is the concentration of water molecules. In Eq. (3), we approximated the exact solution of the heat diffusion equation by an exponential term with the characteristic time T_{cooling} and with β being the ratio between the hypothetical micelle temperature in the absence of heat flux through the membrane and the equilibrated temperature in the focal volume. Although the analytical solutions to the classical heat equation are generally more complex [15], the exponential approximation for micelle cooling is reasonable for our 25-ps experimental window. Slower processes have no relevance to the current study, since the focus is on population relaxation and energy redistribution within the micelle interior. Both of these dynamics are complete in less than 5 ps after the initial excitation. Note that the parameter a in Eq. (2) also accounts for the possible changes in the O–H stretch absorption cross-section due to anharmonic coupling to the intermediate state. At longer delays, this contribution is screened by the much stronger signal originating from the molecules on the hot ground state.

From previous studies of the effect of the hydrogen-bond network on the OH vibrational energy relaxation [21], water molecules in the bulk and water molecules bound to AOT are expected to have different dynamics. The major fraction of the energy that is released by relaxation of AOT-bound water molecules flows directly into nuclear degrees of freedom of the micelle wall. Consequently, this portion does not contribute appreciably to the rise of the water temperature. Hence, the second term in Eq. (3) is governed by the same parameters as for large micelles and bulk water. These considerations significantly reduce the total number of free fitting parameters.

Fig. 4 shows a comparison between several experimental data sets and the model calculations as outlined above for three representative micelle sizes as well as for bulk water. For the smallest micelles ($\mu = 1$), the first term of Eq. (3) dominates because the hot ground state absorption $\sigma_{\text{hot}}(\omega)$ does not differ much from the ground state absorption$\sigma_{01}(\omega)$. Therefore, the pump–probe signal has only a limited sensitivity to the build-up of the hot ground state population as given by Eq. (2). With this in mind, the parameter a is set to zero and the OH-stretching and intermediate mode lifetimes of $T_1 = 800$ fs and $T^* = 450$ fs are obtained directly from the transients. The intermediate mode lifetime is appreciably shorter than the population time T_1 and could therefore only be determined with limited accuracy. Its value of 450 fs turns out to be shorter than the one reported [25] for bulk water (550 fs). This discrepancy might be due to residual bulk-like water molecules whose relaxation prohibits a more accurate determination of the intermediate state lifetime from our data. The cooling time for the smallest micelles is ~2 ps which is consistent with our computer simulations employing the heat-diffusion equation with a source term for heat production that is governed by the above rate equations. This value is also independently confirmed by recording the temperature-driven transient spectrum of the solvent (isooctane) around 3200 cm^{-1} that completely stabilizes by 5 ps. We note that this absorption line presents a convenient means for monitoring the transient temperature outside the smallest micelles. However, for larger micelles its contribution is screened by the much stronger water thermal response in spite of the substantial frequency detuning.

The transient signals obtained for pure water (Fig. 4d) are not influenced by the process of micelle cooling and can therefore provide independent access to the stretching and intermediate mode lifetimes of water molecules involved in the 3D hydrogen-bond network. We

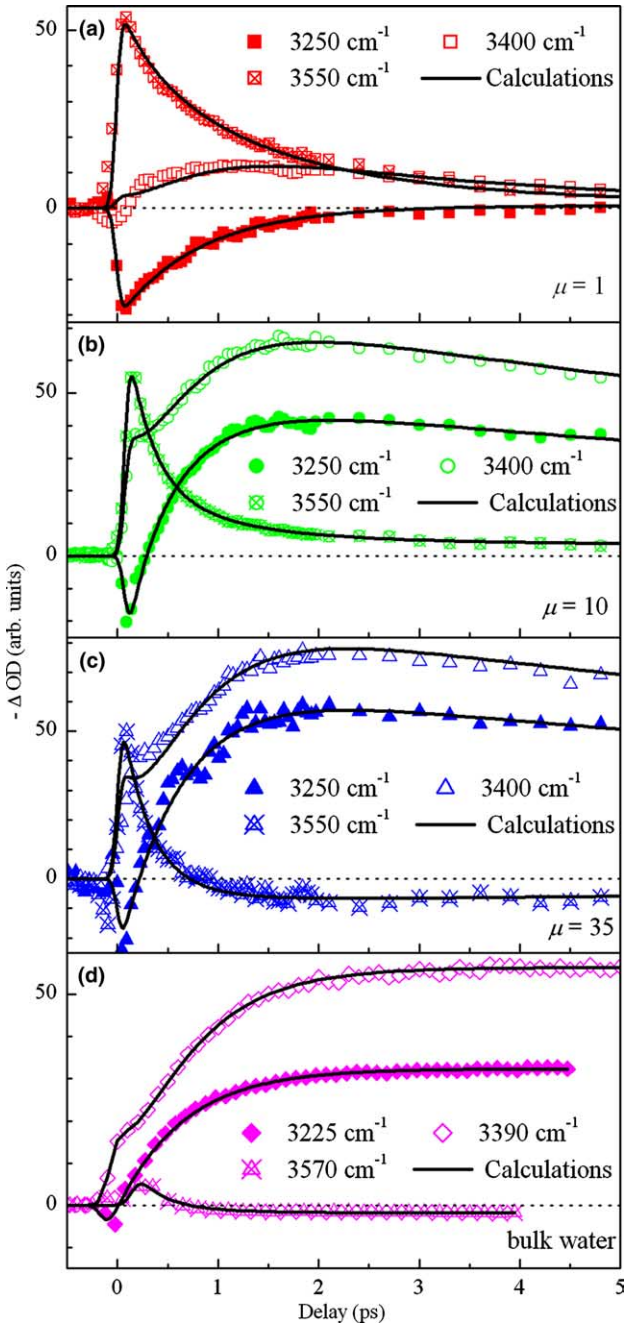

Fig. 4. Typical examples of pump–probe transients for micelles with $\mu = 1$ (a), 10 (b), 35 (c), and bulk water (d). Symbols show the data points at three representative wavelengths while the solid curves depict the results of calculations.

analyzed the data for bulk water together with those for the largest micelles ($\mu = 35$), in which most of the molecules belong to the bulk-like core (Fig. 4c). Both data sets are optimally reproduced with a stretching mode lifetime of T_1=250 fs (270 fs for micelles) which is consistent with the previously reported value of 260 fs [25]. The lifetime of the intermediate state is $T^* = 650$ fs with $a = 0.18$. If a is fixed at zero, a value of $T^* = 550$ fs is recovered, in full accordance with [25]. In this case, however, systematic deviations of the fit from the experimental transients are clearly discernible owing to the excellent signal-to-noise ratio for the bulk water sample. The cooling time for the largest micelles is 8–9 ps.

A controversial discussion concerning OH-stretch population dynamics in liquid water has recently appeared in literature [25–29]. It was argued [26] that the true OH lifetime amounts to ~700 fs while the 250-fs timescale is due to spectral diffusion. Our data acquired with a temporal resolution that is clearly superior to all previous reports, seem to favor an OH-stretch lifetime of 250 fs. Note that the spectrum of our laser pulses uniformly covers the entire absorption band of the OH-stretching mode, thereby minimizing the possible influence of spectral diffusion and/or intraband energy transfer [27]. In addition, a gentle excitation was used to reduce the negative feedback effect, i.e., the prominent dependence of the excited-state lifetime on the temperature jump caused by the already-relaxed OH-oscillators [29]. On the other hand, an assignment of the 650-fs time constant to the build-up time of the hot ground state is strongly supported by the observation that the shape of the transient spectra remains stable from ~0.7 ps onwards. Furthermore, this transient spectrum is identical to the difference of steady-state spectra obtained at room and elevated temperature.

For the intermediate-size micelles ($\mu = 10$), the number of bulk-like water molecules is comparable to the number of AOT-bound molecules. If the model described by Eqs. (1)–(3) is directly applied, a value of $T_1 = 380$ fs is recovered. However, the experimental data points at early time delays are not satisfactorily reproduced. At the blue side of the spectrum, where the pump–probe signal mainly originates from AOT-bound water molecules, the simulations are consistently too fast. In contrast, at the red side where the contribution from bulk-like water dominates, the initial decay of the model calculation is persistently too slow. For this reason, we conclude that the single population lifetime model as given by Eq. (1) fails to adequately describe the experiment. Therefore, a two-component model that accounts for the different population dynamics of the two water sub-ensembles is applied for micelles of intermediate sizes. In this case, the population of the OH-stretching mode (Eq. (1)) is written as the sum of two exponential functions with 250 fs and 800 fs relaxation times, as derived above for the bulk and AOT-bound water species, respectively. Thus, the only free parameters are the amplitudes. As can be seen from Fig. 4b, the experimental data set is perfectly reproduced with such a two-component model, in agreement with previous linear spectroscopy studies on librational motions [30]. In addition, the amplitudes of the two components agree well with the relative amounts of bulk-like and AOT-bound water molecules as determined by MD simulations [7]. The cooling time, T_{cooling}, found for

intermediate-size micelles is, within the experimental uncertainty, equal to that of the largest ones. However, as we mentioned before, this value describes only the initial stages of heat flux away from the micelles.

Finally, we comment on the overall picture of vibrational population dynamics in reverse micelles. The excited state depopulation is noticeably faster for bulk-like water than for AOT-bound water. At the same time, the spectral overlap between the stretching mode and the first overtone of the bending mode at 3300 cm^{-1} [31] is significantly larger for bulk water than for AOT-bound water due to the broader and more red-shifted OH-stretch absorption (Fig. 1) in the former case. These findings support the theory that the first overtone of the bending mode serves as the primary energy acceptor for vibrational relaxation of an initial OH-stretching excitation [21,25,32–34]. On the other hand, the build-up time of the hot-ground state in the large micelles is considerably longer than the relaxation time of the first excited state of the bending mode of ~400 fs obtained for the bulk water [31]. Therefore, if the relaxation of the stretching mode involves the bending mode, the latter does not relax directly to the lower-frequency collective modes like O···O stretch and bend but takes at least one intermediate step, most probably, involving librational modes. Hence, in the model shown in Fig. 3, the intermediate state represents in fact a manifold of states (most probably including bending and librational modes) along which the vibrational relaxation occurs. Additional multi-frequency experiments with a 100-fs resolution are required to reveal all possible relaxation pathways.

In conclusion, femtosecond IR pump–probe spectroscopy has been employed to study vibrational dynamics of water entrapped in reverse micelles with the water droplet diameters ranging from 1 to 10 nm. Our results show that in larger micelles, these dynamics are reminiscent of the bulk phase of liquid water with a fully developed hydrogen-bond network. In the smaller micelles, the hydrogen-bond network is considerably perturbed, which results in an elongated lifetime of the OH-stretching mode of 800 fs. However, this value is still at least an order of magnitude shorter than the corresponding lifetime of an isolated water molecule in liquid solution [21,23]. This suggests that the hydrogen-bond network between water molecules, although weakened in the smallest micelles, still facilitates the population relaxation. One possible scenario involves the intra- (anharmonic) or inter- (Forster-like, [35]) molecular coupling between AOT-bound and water-bound hydroxyl groups with the subsequent relaxation of the latter at the 250-fs time scale. However, our experimental data show no evidence of spectral diffusion and wavelength-dependent lifetime within the O–H stretching band, which are expected in this case. In parallel, the AOT head group may open an additional relaxation channel for water molecules that are bound to the micelle wall [18]. Surprisingly enough, the elementary vibrational dynamics are found to be independent of the micelle size. Rather, the pump–probe data on intermediate-size micelles can simply be understood in terms of two micellar water sub-ensembles, bulk-like and AOT-bound, both independently relaxing according to their own lifetimes for population transfer and energy redistribution. This indicates that the lifetime of the OH-stretching mode is mostly governed by interaction to its closest neighbor be it another water molecule or an AOT head group.

Acknowledgments

This work was supported by the Nederlandse Stichting voor Fundamenteel Onderzoek der Materie (FOM), the Materials Science Centre (MSC) at the University of Groningen, and the Deutsche Forschungsgemeinschaft (Grant No. Vo593/4-1). We thank S. Yeremenko for fruitful discussions.

References

[1] T.K. De, A. Maitra, Adv. Colloid Interf. Sci. 59 (1995) 95.
[2] G.-G. Chang, T.-M. Huang, H.-C. Hung, Proc. Natl. Sci. Counc. ROC B 24 (2000) 89.
[3] M. Li, H. Schnablegger, S. Mann, Nature 402 (1999) 393.
[4] J.-X. Cheng, S. Pautot., D.A. Weitz, X.S. Xie, PNAS 100 (2003) 9826.
[5] P. Hazra, D. Chakrabarty, A. Chakraborty, N. Sarkar, J. Photochem. Photobiol. A 167 (2004) 23.
[6] M.P. Pileni, Structure and Reactivity in Reverse Micelles, Elsevier, Amsterdam, 1989.
[7] J. Faeder, B.M. Ladanyi, J. Phys. Chem. B 104 (2000) 1033.
[8] A. Llor, T. Zemb, in: M.P. Pileni (Ed.), Structure and Reactivity in Reverse Micelles, Elsevier, Amsterdam, 1989, p. 54.
[9] J.E. Boyd, A. Briskman, C.M. Sayes, D. Mittleman, V. Colvin, J. Phys. Chem. B 106 (2002) 6346.
[10] M.R. Harpham, B.M. Ladanyi, N.E. Levinger, K.E. Herwig, J. Chem. Phys. 121 (2004) 7855.
[11] G. Onori, A. Santucci, J. Phys. Chem. 97 (1993) 5430.
[12] D.M. Willard, R.E. Riter, N.E. Levinger, J. Am. Chem. Soc. 120 (1998) 4151.
[13] G.M. Sando, K. Dahl, J.C. Owrutsky, J. Phys. Chem. A 108 (2004) 11209.
[14] Y. Gauduel, A. Migus, J.L. Martin, A. Antonetti, Chem. Phys. Lett. 108 (1984) 319.
[15] T. Patzlaff, M. Janich, G. Seifert, H. Graener, Chem. Phys. 261 (2000) 381.
[16] G. Seifert, T. Patzlaff, H. Graener, Phys. Rev. Lett. 88 (2002) 147402.
[17] E.M. Corbeil, R.E. Riter, N.E. Levinger, J. Phys. Chem. B 108 (2004) 10777.
[18] J.C. Deak, Y. Pang, T.D. Sechler, Z. Wang, D.D. Dlott, Science 306 (2004) 473.
[19] D. Cringus, M.T.W. Milder, M.S. Pshenichnikov, D.A. Wiersma, J. Lindner, P. Vohringer, in: T. Kobayashi, T. Okada, T. Kobayashi, K.A. Nelson, S.D. Silvestri (Eds.), Ultrafast Phenomena XIV, Springer, Niigata, Japan, 2004.

[20] H.S. Tan, I.R. Piletic, R.E. Riter, N.E. Levinger, M.D. Fayer, Phys. Rev. Lett. 94 (2005) 057405.
[21] D. Cringus, S. Yeremenko, M.S. Pshenichnikov, D.A. Wiersma, J. Phys. Chem. B 108 (2004) 10376.
[22] H. Graener, G. Seifert, J. Chem. Phys. 98 (1993) 36.
[23] H. Graener, G. Seifert, A. Laubereau, Chem. Phys. 175 (1993) 193.
[24] R.G. Gordon, J. Chem. Phys. 45 (1966) 1643.
[25] A.J. Lock, H.J. Bakker, J. Chem. Phys. 117 (2002) 1708.
[26] A. Pakoulev, Z. Wang, D.D. Dlott, Chem. Phys. Lett. 371 (2003) 594.
[27] A. Pakoulev, Z. Wang, Y. Pang, D.D. Dlott, Chem. Phys. Lett. 385 (2004) 333.
[28] H.J. Bakker, A.J. Lock, D. Madsen, Chem. Phys. Lett. 385 (2004) 329.
[29] H.J. Bakker, A.J. Lock, D. Madsen, Chem. Phys. Lett. 384 (2004) 237.
[30] D.S. Venables, K. Huang, C.A. Schmuttenmaer, J. Phys. Chem. 105 (2001) 9132.
[31] O.F.A. Larsen, S. Woutersen, J. Chem. Phys. 121 (2004) 12143.
[32] J.C. Deak, S.T. Rhea, L.K. Iwaki, D.D. Dlott, J. Phys. Chem. A 104 (2000) 4866.
[33] A. Pakoulev, Z. Wang, Y. Pang, D.D. Dlott, Chem. Phys. Lett. 380 (2003) 404.
[34] R. Rey, K.B. Moller, J.T. Hynes, Chem. Rev. 104 (2004) 1915.
[35] S. Woutersen, H.J. Bakker, Nature 402 (1999) 507.